

# Simulation and Analysis of the Crankshaft System of the High-Power Marine Engine

**Yang XIAO\***, **Huijun ZHAO\*\***, **Jie WU\*\*\***, **Haibin HE\*\*\***, **Lei WANG\*\*\***, **Hua LOU\*\*\***,  
**Kaimin LIU\*\*\***, **Xiaodong RUAN\*\*\*\***

\*Hangzhou Dianzi University, 1158, 2 Street, Baiyang Street, Qiantang District, Hangzhou 310018, Zhejiang Province, China, E-mail: 21011427@hdu.edu.cn

\*\*Hangzhou Dianzi University, 1158, 2 Street, Baiyang Street, Qiantang District, Hangzhou 310018, Zhejiang Province, China, E-mail: zhaohuijun@hdu.edu.cn (Corresponding author)

\*\*\*Ningbo C.S.I. Power & Machinery Group CO., LTD., 699 Jinshan Road, Jiangbei District, Ningbo 315000, Zhejiang Province, China, E-mails: wujie@ningdong.com, hehaibin@ningdong.com, wanglei@ningdong.com, louhua@ningdong.com, liukaimin@ningdong.com

\*\*\*\*Zhejiang University, 866 Yuhangtang Road, Xihu District, Hangzhou 310012, Zhejiang Province, China, E-mail: xdruan@zju.edu.cn

<https://doi.org/10.5755/j02.mech.38500>

## 1. Introduction

Diesel engine has high thermal efficiency, good adaptability and wide power range, and is the main power source of power machinery in the current national economy and national defense construction. Especially in the Marine transportation industry, high-power diesel engine occupies a dominant position because of its excellent working performance [1-3]. Crankshaft is a key component of diesel engine, which is figuratively likened to the "backbone" of the engine [4]. Its structure is complex, the cost is high, the working environment is harsh, and it is subjected to the effect of bending and torsion alternating load and vibration during the working process. Its performance has a direct impact on the overall performance of the engine [5-9]. With the increasing power of diesel engine, the requirements for crankshaft are more stringent, so the vibration and strength analysis of crankshaft is particularly important [10-12].

In recent years, the maturity of computer technology has enabled the rapid development of finite element method and virtual prototype method, which has made breakthrough progress in the research of dynamic and static characteristics analysis of crankshaft [13-17]. Singh et al. [18] carried out static analysis of the crankshaft of a four-cylinder engine based on ANSYS, and optimized the design of the crankshaft from the aspects of stress and mass. Fonte et al. [19] evaluated the fatigue life of crankshaft of Marine diesel engines and analyzed the possible causes of damage in combination with the example of crankshaft failure. Aliakbari et al. [20] established a non-linear three-dimensional stress analysis model using the elastic-plastic finite element method, estimated the stress field of the crankshaft under cyclic bending load and fixed torsional load, and compared it with the experimental study. Faria et al. [21] developed a program for rapid determination of fatigue strength of crankshaft through thermal imager method, which can replace traditional fatigue measurement methods and improve the efficiency of evaluating fatigue strength of crankshaft. Baragetti et al. [22] studied the influence of residual stress after crankshaft nitriding treatment on fatigue strength through numerical simulation and test, and proposed a method to measure residual stress

of crankshaft by bending strain measurement. Ding et al. [23] adopted professional programming software to realize dynamic calculation and analysis of diesel engine crankshaft on the basis of traditional algorithms, calculated the bending and torsional load of crankshaft, and checked the fatigue strength of crankshaft. Fu et al. [24] established a finite element model with ANSYS to study the deformation and stress of the crankshaft and conduct modal analysis of the crankshaft, providing sufficient theoretical basis for the optimization design of the engine. Wang et al. [25] used EXCIT software to establish a flexible multi-body dynamic coupling model, carried out high-cycle fatigue analysis according to the dynamic calculation results, and calculated the crankshaft safety factor to check the crankshaft strength. Qin et al. [26] put forward the simulation method and theory of the quenching process to analyze the fatigue strength of the crankshaft section, and the calculated results are consistent with the resonance bending fatigue test of the crankshaft section. With the continuous development of diesel engine to reduce fuel consumption, pollution and noise, improve working reliability and prolong service life, the study of diesel engine crankshaft static and dynamics has important engineering significance and application value.

In this paper, the crankshaft system of NL9340 high-power diesel engine was as the research object. Firstly, three-dimensional modeling is carried out, and then the inherent frequency and vibration mode of the crankshaft are calculated through the finite element free mode simulation analysis. On this basis, the rigid-flexible coupling finite element simulation model of the crankshaft system is established, and the dynamic and kinematic simulation analysis of the crankshaft system is carried out. By using the calculated pressure load spectrum of the crankshaft in the steady state process, the boundary conditions are set up, and the static simulation model of the crankshaft is established to simulate and analyze its static strength. The study of the dynamic and static characteristics of the crankshaft system of high-power diesel engine can provide reference for the optimization of the crankshaft structure, and provide reference for the economic and reliability design of the crankshaft.

## 2. Crankshaft Finite Element Modeling

The crankshaft structure of NL9340 high-power diesel engine is a straight nine-cylinder layout, which is composed of nine single turn crankshaft, free end and output end. The crankshaft geometric model of the crankshaft is shown in Fig. 1. Tetrahedral mesh was adopted, and the mesh of key parts such as the transition corner between the shaft neck and the crank arm was refined. The mesh size was set to 50 mm, the total mesh number was 55781, and



Fig. 1 The crankshaft geometry model

the number of nodes was 89611. The crankshaft material is 42CrMo with a density of 7850 kg/m<sup>3</sup>, A Poisson's ratio of 0.28 and an elastic modulus of 212 GPa.

## 3. Crankshaft Free Mode Analysis

Engine resonance is usually easier to occur at low order frequencies, so the frequency and patterns of the first 14 order harmonics were calculated. Since the inherent frequency of the first 6th order modes is almost 0, it can be regarded as a rigid body mode, and the non-zero first order mode is actually the 7th order mode. The inherent frequency and mode characteristics of each mode of the crankshaft order 7-14 are shown in Table 1. The inherent frequency of the non-zero mode of the crankshaft is in the range of 21-125 Hz.

The order 7-14 mode of crankshaft is shown in Fig. 2, where the coordinate system X direction is the vertical direction of piston movement, Y direction is perpendicular to the vertical motion direction, and Z direction is the direction of the crankshaft axis. The vibration modes of

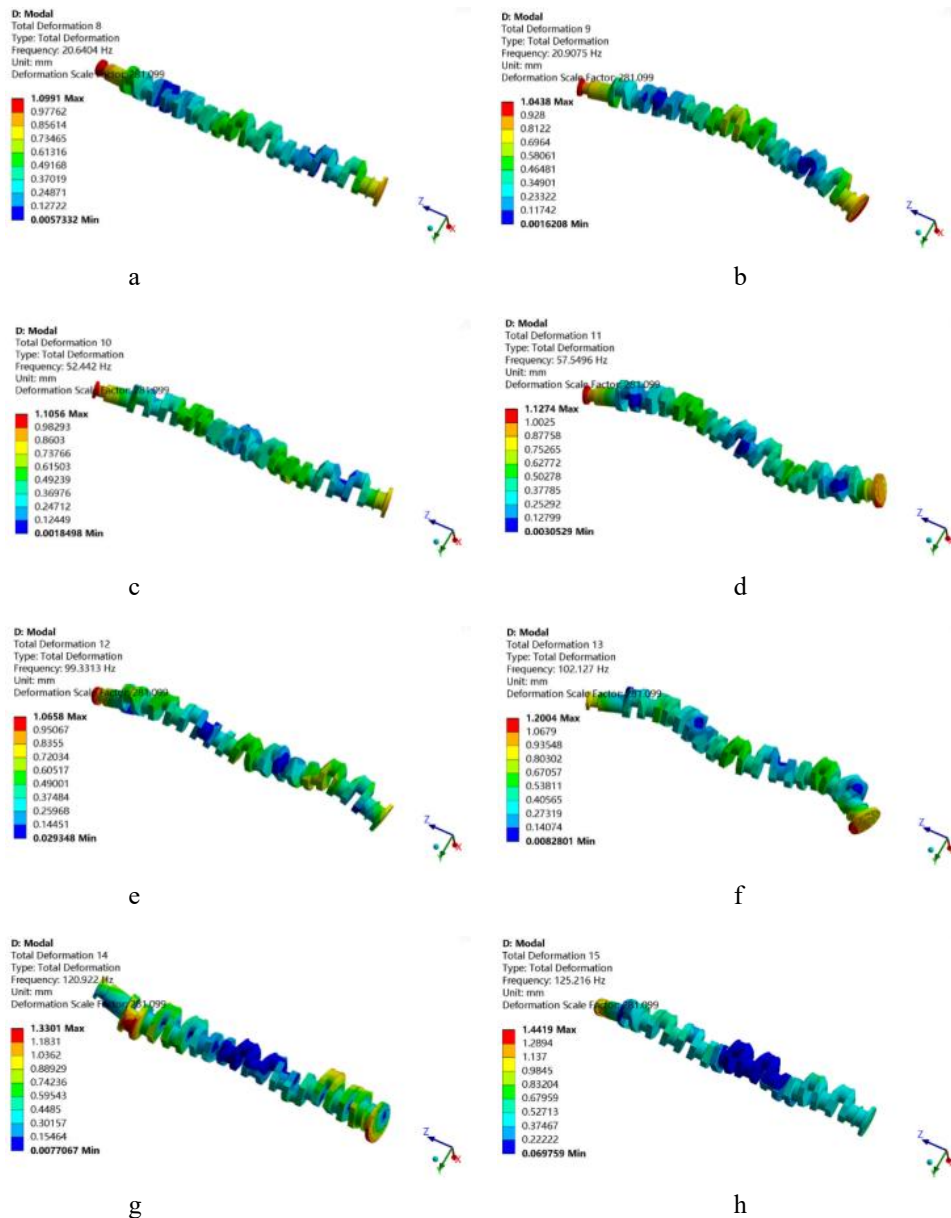


Fig. 2 Crankshaft mode diagrams: a – the 7th order, b – the 8th order, c – the 9th order, d – the 10th order, e – the 11th order, f – the 12th order, g – the 13th order, h – the 14th order

Table 1  
Crankshaft inherent frequency and vibration pattern

Mode order	Inherent frequency, Hz	Mode characteristics
7	20.640	First-order bending vibrations in the YOZ plane
8	20.907	First-order bending vibrations in the XOZ plane
9	52.442	Second-order bending vibrations in the YOZ plane
10	57.550	Second-order bending vibrations in the XOZ plane
11	99.331	Coupling vibration of third-order bending in the XOZ plane and twisting around the Z-axis
12	102.130	Coupling vibration of third-order bending in the YOZ plane and twisting around the Z-axis
13	120.920	Coupling vibration of second-order bending in the YOZ plane and twisting around the Z-axis
14	125.220	Coupling vibration of second-order bending in the XOZ plane and twisting around the Z-axis

the lower order 7-10 are mainly the first or second order bending vibration in the plane, while the vibration modes

of the order 11-14 are the coupling vibration of bending in the plane and torsion around the Z axis.

#### 4. Analysis of Dynamics in the Crankshaft System

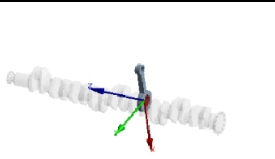
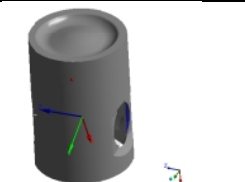
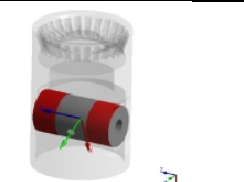
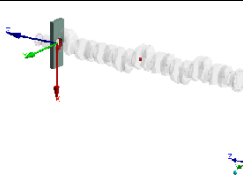
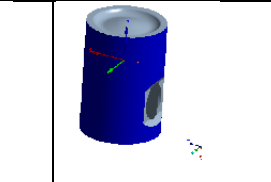
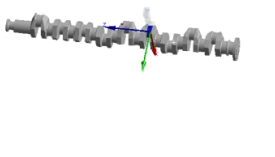

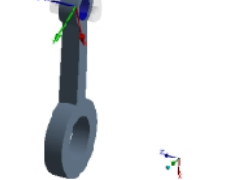
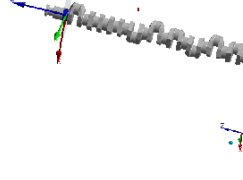
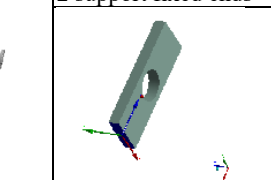
##### 4.1. Rigid-flexible coupling finite element modeling

In this paper, the flexible treatment of the crankshaft was carried out, and the dynamic model of the crankshaft system is shown in Fig. 3. According to the actual movement of the crankshaft system, 9 connections between the camshaft journal and the connecting rod rotating pair, 9 connections between the outer end of the pin shaft and the piston rotating pair, 9 connections between the middle section of the pin shaft and the connecting rod rotating pair, 2 connections between the support bearing and the camshaft journal rotating pair, 2 cylindrical pairs between the piston and the fixed end, and 2 support fixed ends. The specific constraints and support conditions are shown in Table 2.

To set the boundary conditions of the crankshaft system, the pressure curve in the cylinder during the working cycle must be obtained. In this paper, the rated speed is 650 r/min, the rated power is 5400 kW, and 100 % of the load is used. Take the rotation Angle of 0.5 ° crankshaft as the step length, and measure the crankshaft rotation of 720 °, that is, the curve of the gas pressure in the engine cylinder in a working cycle with the angle changes, as shown in Fig. 4.

Table 2

The specific constraints and support conditions

9 connections between the camshaft journal and the connecting rod rotating pair	9 connections between the outer end of the pin shaft and the piston rotating pair	9 connections between the middle section of the pin shaft and the connecting rod rotating pair	2 connections between the support bearing and the camshaft journal rotating pair	2 cylindrical pairs between the piston and the fixed end
				
				2 support fixed ends
				

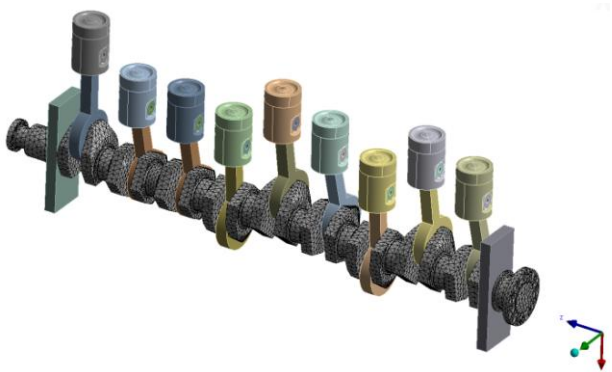


Fig. 3 Rigid-flexible coupling finite element model of the crankshaft system

According to the ignition sequence 1-6-8-2-5-7-3-4-9 of NL9340 high-power diesel engine, the aerodynamic force as an external load is loaded on the

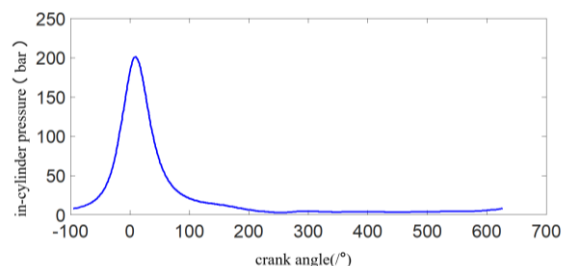


Fig. 4 In-cylinder pressure curve under rated engine condition

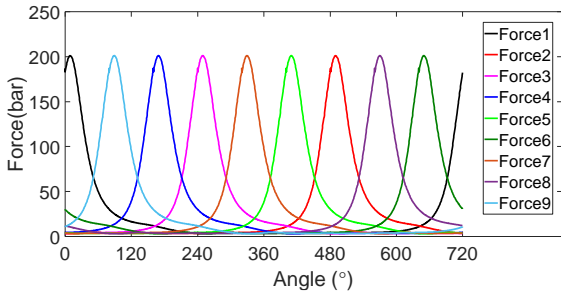


Fig. 5 Pressure curve of each cylinder under rated engine condition

top of each piston along the direction of the cylinder axis. The pressure curve of 9 cylinders of the engine under rated working conditions is shown in Fig. 5. The rotation speed was created on the crankshaft rotation pair to set the engine to run at 650 r/min, converted to 68.03 rad/s, with a calculation time of 0.18462 s. The explicit dynamic analysis was used for the solver. To improve the convergence of simulation calculation, the initial step was set to  $5 \times 10^{-5}$ , the minimum step was set to  $1 \times 10^{-10}$ , and the maximum step was set to  $5 \times 10^{-5}$ .

4.2. Analysis of the crankshaft system dynamics

In the rigid and flexible coupling model, the piston and piston connecting rod are rigid, and the crankshaft is flexible, so under the action of external load, the connecting rod and piston will not deform, but the crankshaft, as a flexible long rod, will bend and twist deformation under the action of the external load. Fig. 6 shows the force diagram of the connecting rod journal. It can be seen that the load spectrum amplitude of the connecting rod journal

1 to 9 mainly fluctuates within the range of 20000 kN in one working cycle of the engine.

The maximum exciting force load of each journal can be known from the obtained load spectrum of connecting rod journal. The maximum exciting force of the connecting rod journal is about 20000-30000 kN, of which the first connecting rod journal and the second connecting rod journal are subjected to significant loads, the maximum exciting force of the first connecting rod journal is 33665 kN, the maximum exciting force of the second connecting rod journal is 30674 kN, the maximum exciting force of the third connecting rod journal is 19379 kN, and the force is the least. The maximum exciting force of the fourth link journal is 21308 kN, the maximum exciting force of the fifth link journal is 23341 kN, the maximum exciting force of the sixth link journal is 20054 kN, the maximum exciting force of the seventh link journal is 26214 kN, the maximum exciting force of the eighth link journal is 26127 kN, and the maximum exciting force of the ninth link journal is 26283 kN.

Fig. 7 shows the force diagram of nine piston pins. It can be seen that the load of each piston pin mainly fluctuates within the range of 20000 kN, and the force of the first piston pin and the second piston pin is the most obvious.

4.3. Kinematic analysis of the crankshaft system

Fig. 8 and Fig. 9 are the displacement curves and velocity curves of the nine pistons respectively. It can be seen from the figure that the trend of the displacement curve of each piston shows a periodic simple harmonic curve, and the trend of the speed curve of each piston

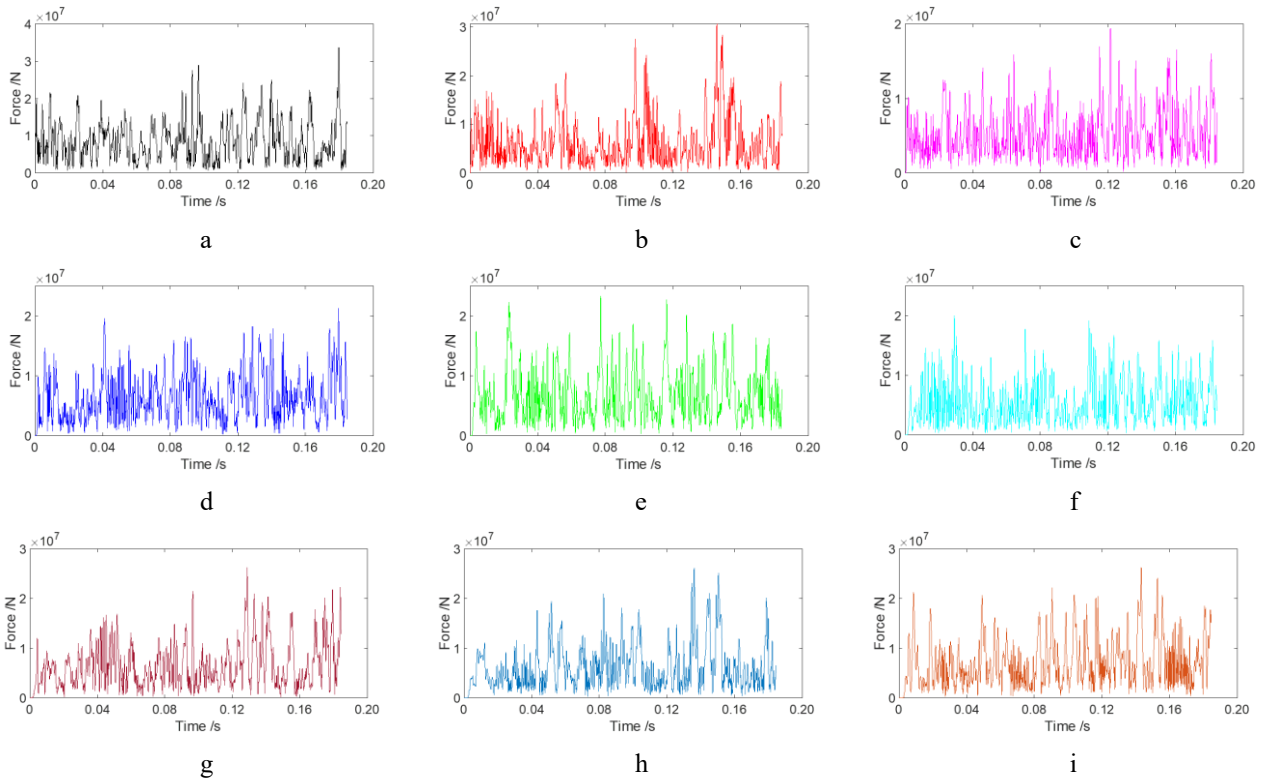


Fig. 6 Force diagrams of connecting rod journal: a – first connecting rod journal, b – second connecting rod journal, c – third connecting rod journal, d – fourth connecting rod journal, e – fifth connecting rod journal, f – sixth connecting rod journal, g – seventh connecting rod journal, h – eighth connecting rod journal, i – ninth connecting rod journal

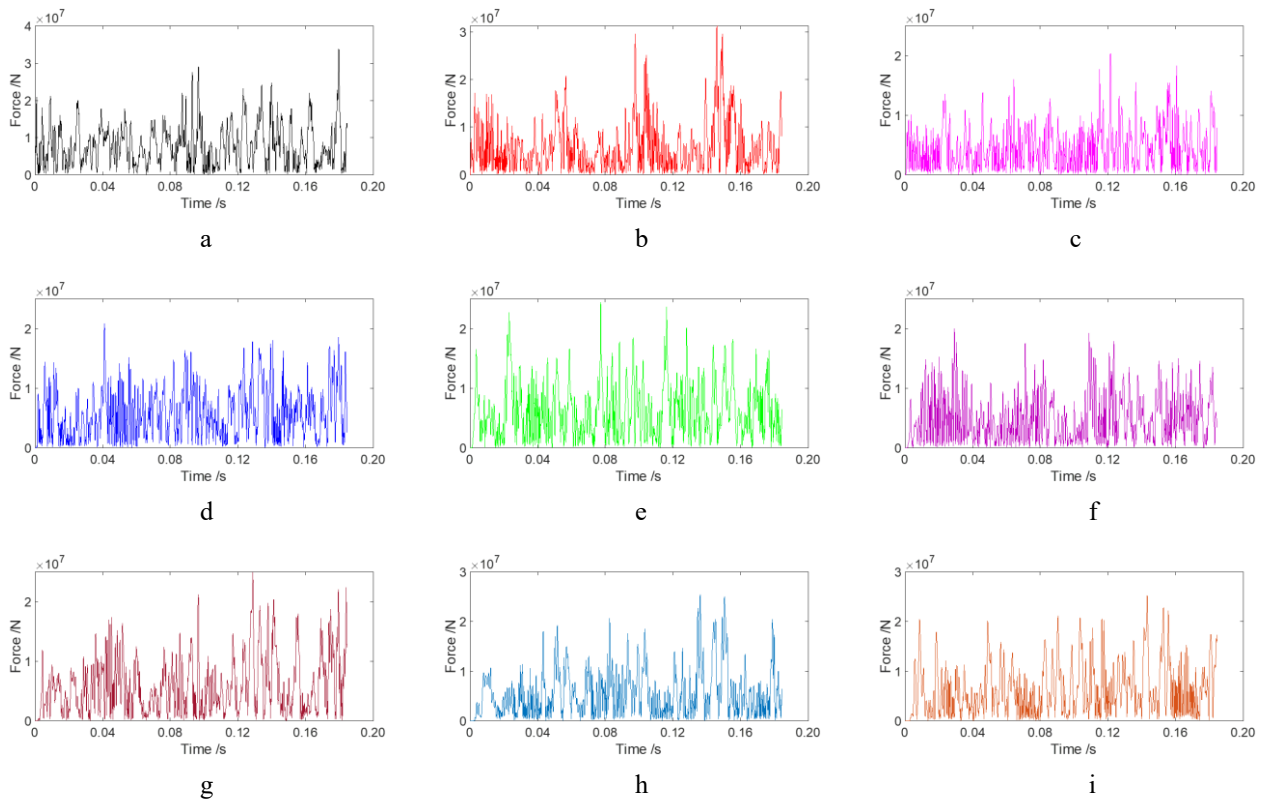


Fig. 7 Piston pin force diagrams: a – piston pin 1, b – piston pin 2, c – piston pin 3, d – piston pin 4, e – piston pin 5, f – piston pin 6, g – piston pin 7, h – piston pin 8, i – piston pin 9

generally presents a periodic change law. Because the diesel engine is in-line nine cylinder, according to the ignition order of the engine, the movement of piston 2 and 3 is basically the same, the movement of piston 4 and 7 is basically the same, the movement of piston 5 and 8 is basically the same, the movement of piston 6 and 9 is basically the same, the minimum displacement of each piston is 29 mm, the maximum displacement is 543 mm. The maximum piston speed can reach 38835 mm/s.

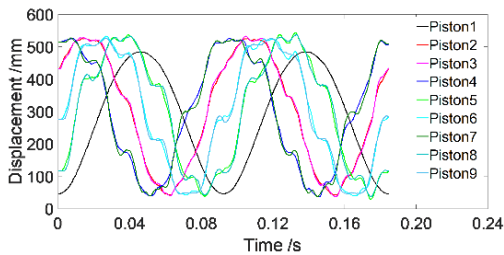


Fig. 8 The piston displacement curves

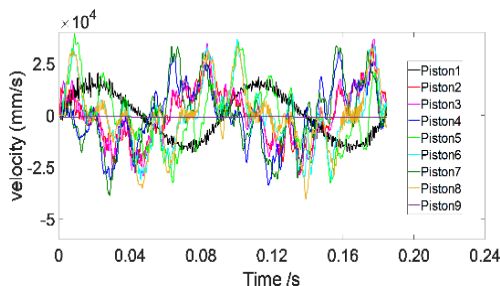


Fig. 9 The piston velocity curves

Fig. 10 shows the acceleration curve of the nine pistons. It can be seen that the acceleration of each piston

fluctuates within the range of  $3 \times 10^7 \text{ mm/s}^2$  in general. Piston 1 shows a maximum acceleration of  $2.98 \times 10^7 \text{ mm/s}^2$ , Piston 2 is of a maximum acceleration of  $2.91 \times 10^7 \text{ mm/s}^2$ , A maximum acceleration of piston 3 is  $2.75 \times 10^7 \text{ mm/s}^2$ , The maximum acceleration of piston 4 is  $1.95 \times 10^7 \text{ mm/s}^2$ , Piston 5 has a maximum acceleration of  $2.43 \times 10^7 \text{ mm/s}^2$ , Piston 6 is of a maximum acceleration of  $1.96 \times 10^7 \text{ mm/s}^2$ , Piston 7 has a maximum acceleration of  $2.37 \times 10^7 \text{ mm/s}^2$ , Piston 8 has a maximum acceleration of  $1.97 \times 10^7 \text{ mm/s}^2$ , Piston 9 is of a maximum acceleration of  $2.93 \times 10^7 \text{ mm/s}^2$ .

## 5. Crankshaft Static Mechanical Analysis

According to the finite width oil film distribution law, the maximum load value of each cylinder of the engine was applied to the connecting rod journal by using the load spectrum obtained by dynamic simulation. Fig. 11 is the equivalent stress distribution cloud diagram of the crankshaft. It can be seen that the stress is the greatest and most concentrated at the over-rounded corner between the connecting rod journal and the crank, followed by the over-rounded corner between the main journal and the crank, indicating that the crankshaft is most prone to failure in these areas. It can be seen from the cloud diagrams of the local equivalent stress of each cylinder of the crankshaft that the equivalent stress at the second cylinder is the largest, and the equivalent stress value is 14.103 MPa

The deformation cloud map of the crankshaft is shown in Fig. 12. It can be seen that the average deformation of the crankshaft is  $4.4703 \times 10^{-3} \text{ mm}$  and the maximum deformation is  $8.3683 \times 10^{-3} \text{ mm}$ , which appears at the neck of the second cylinder connecting rod. The other places with a larger deformation are the necks of the fifth and sixth cylinder connecting rod, respectively.



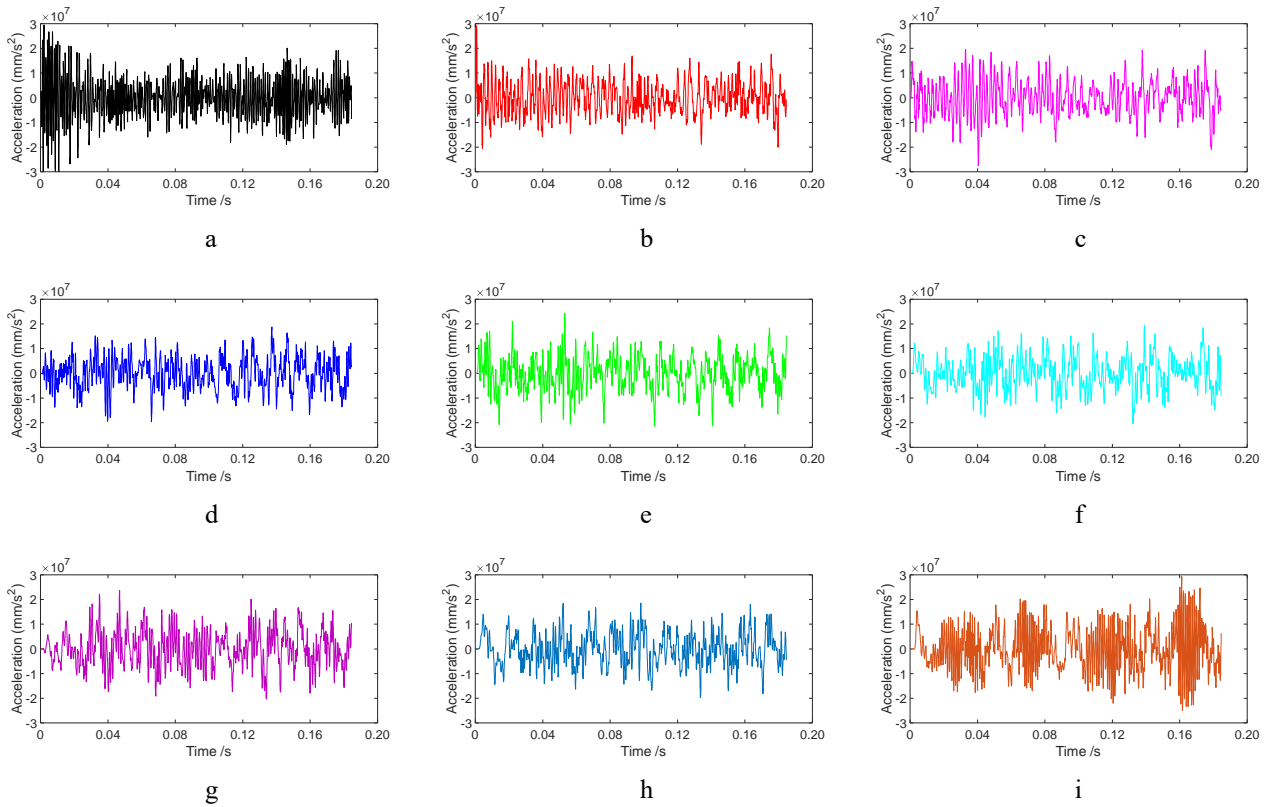


Fig. 10 The piston acceleration curves: a – piston 1, b – piston 2, c – piston 3, d – piston 4, e – piston 5, f – piston 6, g – piston 7, h – piston 8, i – piston 9

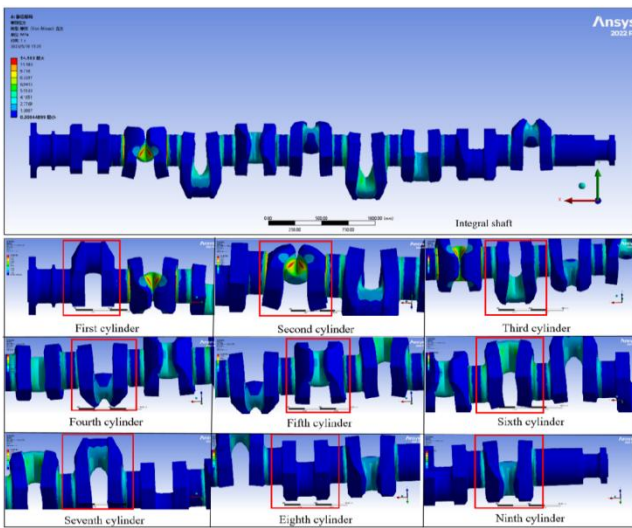


Fig. 11 Crankshaft equivalent stress distribution

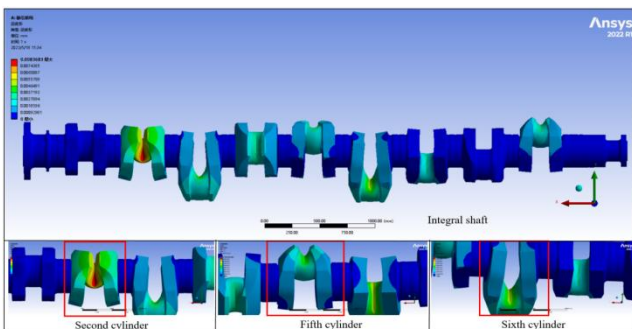


Fig. 12 Crankshaft deformation cloud diagrams

## 6. Conclusions

In this paper, the NL9340 high-power diesel engine crankshaft system was studied by statics and dynamics simulation. The conclusions are as follows.

The finite element free mode simulation model of the crankshaft was established, and the inherent frequencies and vibration modes of the first 14 harmonics of the crankshaft were calculated. The results show that the inherent frequency of the non-zero mode of the crankshaft is in the range of 21-125 Hz, and its mode is mainly manifested as the bending vibration in the plane or the coupling vibration of bending in the plane and torsion around the Z axis.

The rigid-flexible coupling finite element model of the crankshaft system was established. Through the dynamic simulation of the crankshaft system, it was calculated that the load spectrum of each cylinder connecting rod journal and piston pin mainly fluctuates within the range of 20000 kN, in which the first connecting rod journal and the second connecting rod journal have obvious forces, and the maximum exciting force is above 30000 kN. The kinematic characteristics of displacement, velocity and acceleration of each piston are analyzed.

The static simulation model of the crankshaft was established, and the results show that the stress is the largest force and most concentrated at the over-rounded corner between each connecting rod journal and crank, and the maximum equivalent stress and deformation occur at the second cylinder connecting rod journal, which are 14.103 MPa and  $8.3683 \times 10^{-3}$  mm respectively.

## Funding

This study was supported by the "Pioneer" R&D Program of Zhejiang (Grant No. 2024C01038).

## Author Contributions

**Yang Xiao:** Methodology, Formal analysis, Data curation, Writing – original draft. **Huijun Zhao:** Conceptualization, Methodology, Funding acquisition, Writing – original draft. **Jie Wu:** Conceptualization, Funding acquisition, Writing – review & editing. **Haibin He:** Conceptualization, Validation, Writing – original draft. **Lei Wang:** Methodology, Writing – review & editing. **Hua Lou:** Validation, Writing – review & editing. **Kaimin Liu:** Formal analysis, Writing – review & editing. **Xiaodong Ruan:** Methodology, Writing – review & editing. All authors have read and agreed to the published version of the manuscript.

## References

- Dabilgou, T.; Tubreoumya, G. C.; Haro, K.; Zongo, S.; Kam, S. Z.; Sandwidi, S.; Ouédraogo, T. L.; Daho, T.; Koulidiati, J.; Sanogo, O.; Zeghmati, B.; Bere, A.** 2021. Review and Synthesis of Literature on Single and Multizone Thermodynamic Combustion in a Diesel Engine, *Physical Science International Journal* 25(12): 1-14. <https://doi.org/10.9734/psij/2021/v25i1230294>.
- Liu, Y.; Kuznetsov, A.; Sa, B.** 2021. Simulation and Analysis of the Impact of Cylinder Deactivation on Fuel Saving and Emissions of a Medium-Speed High-Power Diesel Engine, *Applied Sciences* 11(16): 7603. <https://doi.org/10.3390/app11167603>.
- Jin, J.; Wang, J.; Zhang, C.; Cao, T.** 2024. Review of Research on Asymmetric Twin-Scroll Turbocharging for Heavy-Duty Diesel Engines, *SAE International Journal of Commercial Vehicles* 17(2): 147-163. <https://doi.org/10.4271/02-17-02-0009>.
- Abdel-Salam, A. S. G.; Sohail, A.; Sherin, L.; Azim, Q. U. A.; Faisal, A.; Fahmy, M. A.; Li, Z.** 2023. Optimization of tank engine crank shaft material properties, *Mechanics Based Design of Structures and Machines* 51(6): 3066-3082. <https://doi.org/10.1080/15397734.2021.1916754>.
- Xue, Z. J.; Han, M. B.** 2023. Crack analysis of crankshaft for diesel engine, *Metalurgija* 62(2): 296-298. Available at: <https://hrcaak.srce.hr/290119>.
- Oral, A.; Subasi, O.; Sahin, C.; Ul Haque, U.; Lazoglu, I.** 2023. Effect of starting position of crankshaft on transient body vibrations of reciprocating compressor, *International Journal of Refrigeration* 149: 135-145. <https://doi.org/10.1016/j.ijrefrig.2022.12.028>.
- Qin, W. J.; Dong, C.; Li, X.** 2016. Assessment of Bending Fatigue Strength of Crankshaft Sections with Consideration of Quenching Residual Stress, *Journal of Materials Engineering and Performance* 25(3): 938-947. <https://doi.org/10.1007/s11665-016-1890-1>.
- Li, J.; Zuo, Z.; Jia, B.; Feng, H.; Wei, Y.; Zhang, Z.; Smallbone, A.; Roskilly, A. P.** 2021. Comparative analysis on friction characteristics between free-piston engine generator and traditional crankshaft engine, *Energy Conversion and Management* 245: 114630. <https://doi.org/10.1016/j.enconman.2021.114630>.
- Mendes, A.; Kanpolat, E.; Rauschen, R.** 2013. Crankcase and Crankshaft Coupled Structural Analysis Based on Hybrid Dynamic Simulation, *SAE International Journal of Engines* 6(4): 2044-2053. <https://doi.org/10.4271/2013-01-9047>.
- Li, H.; Liu, F.; Kong, X.; Zhang, J.; Jiang, Z.; Mao, Z.** 2023. Knowledge features enhanced intelligent fault detection with progressive adaptive sparse attention learning for high-power diesel engine, *Measurement Science and Technology* 34(10): 105906. <https://doi.org/10.1088/1361-6501/ace278>.
- Feese, T.; Hill, C. L.** 2009. Prevention of torsional vibration problems in reciprocating machinery, *Turbomachinery and Pump Symposia* (38th): 213-238. <https://doi.org/10.21423/R1XP9Z>.
- Rödling, S.; Fröschl, J.; Decker, M.** 2012. Experimental Fatigue Assessment of Crankshafts: Presentation of a Damage Equivalent Component Test Method, *Materials Testing* 54(10): 648-654. <https://doi.org/10.3139/120.110383>.
- Azzawi, M. M.; Hadi, A. S.; Abdullah, A. R.** 2023. Finite Element Analysis of Crankshaft Stress and Vibration in Internal Combustion Engines Using ANSYS, *Mathematical Modelling of Engineering Problems* 10(3): 1011-1016. <https://doi.org/10.18280/mmep.100335>.
- Xu, Y. M.; Teng, X. B.** 2024. Investigation of the lubrication performance of a marine diesel engine crankshaft using a thermo-electrohydrodynamic model, *Non-linear Engineering* 13(1): 2024002. <https://doi.org/10.1515/nleng-2024-0002>.
- Mendes, A. S.; Meirelles, P. S.; Zampieri, D. E.** 2008. Analysis of torsional vibration in internal combustion engines: modelling and experimental validation, *Proceedings of the Institution of Mechanical Engineer, Part K: Journal of Multi-body Dynamics* 222(2): 155-178. <https://doi.org/10.1243/14644193JMBD126>.
- Zhang, Q.; Wang, D.; Zhang, K.; Fang, Z.; Yin, X.; Liu, J.** 2024. COMSOL-based fatigue simulation of crankshaft, *Journal of Physics: Conference Series* 2741: 012025. <https://doi.org/10.1088/1742-6596/2741/1/012025>.
- Lu, J.; Zheng, H.; Haider, M. H.; Feng, Y.; Zhi, P.; Cheng, J.; Wang, Z.** 2023. Fracture failure analysis of flywheel hub served in heavy-fuel aviation piston engine, *Engineering Failure Analysis* 151: 107363. <https://doi.org/10.1016/j.engfailanal.2023.107363>.
- Singh, A.; Mittal, V. K.; Angra S.** 2014. Strength Analysis and Optimization Methods for four Cylinder Engine Crankshaft Based on CATIA and ANSYS, *Applied Mechanics and Materials* 592-594: 1789-1793. <https://doi.org/10.4028/www.scientific.net/AMM.592-594.1789>.
- Fonte, M.; Duarte, P.; Anes, V.; Freitas, M.; Reis, L.** 2015. On the assessment of fatigue life of marine diesel engine crankshafts, *Engineering Failure Analysis* 56: 51-57. <https://doi.org/10.1016/j.engfailanal.2015.04.014>.
- Aliakbari, K.** 2021. Failure Analysis of Ductile Iron Crankshaft in Four-Cylinder Diesel Engine, *Internation*

- tional Journal of Metalcasting 15(4): 1223-1237.  
<https://doi.org/10.1007/s40962-020-00550-y>.
21. **Faria, J. J. R.; Fonseca, L. G. A.; de Faria, A. R.; Cantisano, A.; Cunha, T. N.; Jahed, H.; Montesano, J.** 2022. Determination of the fatigue behavior of mechanical components through infrared thermography, *Engineering Failure Analysis* 134: 106018.  
<https://doi.org/10.1016/j.engfailanal.2021.106018>.
  22. **Baragetti, S.; Cavalleri, S.; Terranova, A.** 2010. Numerical and Experimental Investigation on the Fatigue Behavior of a Steel Nitrided Crankshaft for High Power IC Engines, *Journal of Engineering Materials and Technology-Transactions of the ASME* 132(3): 031014.  
<https://doi.org/10.1115/1.4001834>.
  23. **Ding, Y.; Sui, C. B.; Yao, Y.** 2013. Dynamic Crankshaft Strength Calculation of Diesel Engine using Simulation Techniques, *Advanced Materials Research* (860-863): 1699-1702.  
<https://doi.org/10.4028/www.scientific.net/AMR.860-863.1699>.
  24. **Fu, Z. M.** 2011. FEM Analysis of Engine Crankshaft Static and Dynamic Behaviour Using ANSYS, *Applied Mechanics and Materials* (121-126): 3315-3319.  
<https://doi.org/10.4028/www.scientific.net/AMM.121-126.3315>.
  25. **Wang, L. J.; Li, D.; Lu, X. X.; Li, P. F.; Jia, Y. J.** 2014. Strength Analysis of Diesel Engine Crankshaft Based on Flexible Multi-Body Dynamics, *Applied Mechanics and Materials* 654: 65-68.  
<https://doi.org/10.4028/www.scientific.net/AMM.654.65>.
  26. **Qin, W. J.; Dong, C.; Li, X.** 2016. Assessment of Bending Fatigue Strength of Crankshaft Sections with Consideration of Quenching Residual Stress, *Journal of Materials Engineering and Performance* 25(3): 938-947.  
<https://doi.org/10.1007/s11665-016-1890-1>.

Y. Xiao, H. Zhao, J. Wu, H. He, L. Wang, H. Lou, K. Liu, X. Ruan

#### SIMULATION AND ANALYSIS OF THE CRANK-SHAFT SYSTEM OF THE HIGH-POWER MARINE ENGINE

#### S u m m a r y

The crankshaft is one of the most important parts of the engine and is likened to the "backbone" of the engine. In this paper, NL9340 high power diesel engine crankshaft system as the research object, the finite element free mode simulation model of crankshaft was established, and the inherent frequency and vibration mode of crankshaft were calculated. Through the rigid-flexible coupling finite element simulation of the crankshaft system, the dynamic and kinematic characteristics of the crankshaft system were analyzed. It was calculated that the load spectrum of each cylinder connecting rod journal and piston pin mainly fluctuated in the range of 20000 kN, in which the maximum exciting forces of the first connecting rod journal and the second connecting rod journal are above 30000 kN. On this basis, the static strength of the crankshaft was simulated and analyzed. The results show that the stress is the greatest and most concentrated at the over-rounded corner between connecting rod journal and crank. The maximum equivalent stress and deformation occur at the second cylinder connecting rod journal, which are 14.103 MPa and  $8.3683 \times 10^{-3}$  mm respectively.

**Keywords:** crankshaft, modal analysis, rigid-flexible coupling model, dynamic simulation, statics simulation.

Received August 16, 2024

Accepted December 16, 2024



This article is an Open Access article distributed under the terms and conditions of the Creative Commons Attribution 4.0 (CC BY 4.0) License (<http://creativecommons.org/licenses/by/4.0/>).